



Dynamics of Eclipse Environment: Cut-off Frequency and Orbital Phase Dependent Polarization Study for PSR J0024–7204 and PSR J1431–4715

Sangita Kumari⁽¹⁾, Bhaswati Bhattacharyya^{*(1)}
(1) National Centre for Radio Astrophysics, Pune, India

Abstract

In majority of the black widow (BW) millisecond pulsar systems (MSPs), the cyclotron synchrotron mechanism is thought to be responsible for the observed frequency dependent eclipses implying the presence of magnetic field in the eclipse environment. We present an orbital phase-dependent study of two BW MSPs to explore the magnetic field in the eclipse environment using full polar observations from the Parkes Telescope's ultra wide-band low frequency (UWL) receiver covering frequencies from 704 MHz to 4032 MHz. We observed depolarisation of pulses during the eclipse phase for two BW MSPs, J0024–7204 and J1431–4715, as has been seen in other such systems. We determined the non eclipse phase RM of $+20 \text{ rad/m}^2$ and $+30 \text{ rad/m}^2$ for PSR J0024–7204 and PSR J1431–4715 respectively. While studying the frequency dependent eclipsing for these BW MSPs we obtained constraints on the cut-off frequency. For PSR J0024–7204 we found an indication of eclipse cut-off frequency varying with time, along with changes in the electron column density in the eclipse medium for a sample of six eclipses. Additionally, we determined the eclipse cut-off frequency for PSR J1431–4715 to be $1251 \pm 80 \text{ MHz}$ and conclude that synchrotron absorption is the primary mechanism responsible for the eclipse.

1 Introduction

Eclipsing spider MSPs are compact binaries in which the energetic pulsar wind ablates the companion and this ablated material is assumed to be the cause of observed eclipses (e.g. $\sim 10\%$ of the binary orbit is eclipsed for PSR J1959+2048, 1). Based on the mass of the companion (M_c), spider MSPs are divided into two categories: black widow (BW, $M_c < 0.05M_\odot$, 2) and redback (RB, $0.1M_\odot < M_c < 0.9M_\odot$, 2). Owing to the frequency-dependent nature of the eclipses, the pulsed signal from the pulsar disappears within the eclipse region below a certain frequency called the eclipse cut-off frequency (ν_c).

Polarization studies in BW MSPs with eclipses are crucial for determining the magnetic field in the eclipse medium, which plays a significant role in understanding the eclipse mechanism (e.g. 9; 16). An in-depth exploration of potential eclipse mechanisms is provided by (5), offering explanations for the frequency-dependent eclipses in spider

MSP systems. Previous studies by (6), (7) and (8) found cyclotron-synchrotron absorption to be the primary mechanism for eclipses in PSR J1227–4853, PSR J1544+4937 and PSR J1810+1744 respectively. Scattering and cyclotron absorption are considered as the main mechanisms for PSR J2051–0827 (9). By estimating the magnetic field in the eclipse medium, one can gain valuable insights into whether cyclotron or synchrotron absorption is responsible for the observed eclipses in these systems, which have hitherto been unexplored. We have selected two BW MSPs namely, J0024–7204 and PSR J1431–4715. For these MSPs, orbital phase-dependent polarization study has not been conducted previously, and their Parkes UWL data is publicly available. The UWL receiver at the Parkes Telescope offers a wide bandwidth covering frequencies from 704 MHz to 4032 MHz, which is useful for identifying the cut-off frequency and studying its corresponding temporal variations in the spider system. Simultaneous polarization observations also provide a platform for the polarimetric study of these systems.

2 Results

We analyzed the folded mode data available in the CSIRO data archive¹ for PSR J0024–7204 and J1431–4715 (details in Table 1). We analyzed the data using PSRCHIVE. For the subsequent study, we utilized the calibrated profiles for each pulsar, including 4 Stokes parameters, 104 frequency channels across the observing bandwidth, and 512 phase bins.

2.1 Temporal variation of ν_c ?

We estimated the eclipse cut-off frequency for PSR J0024–7204 and J1431–4715, as listed in Table 1. The temporal variation of the cut-off frequency for PSR J0024–7204 is implied from Table 1. Previous studies reported a complete eclipse at 440 MHz, a variable eclipse at 660 MHz, and no detectable eclipse at 1400 MHz (11). For PSR J1431–4715, we determined the cut-off frequency to be 1251 MHz. In the previous study by (12), a signature of eclipsing is observed in the timing residuals at 700 MHz and 1400 MHz. The radio signal never disappeared in the eclipse region, but a delay was seen at 700 MHz and 1400 MHz. Our estimate of the cut-off frequency at 1251

¹<https://data.csiro.au>

MHz suggests that the cut-off frequency could be varying with time. Temporal changes in the cut-off frequency have been reported for PSR J1544+4937 by (10), depicting the dynamical evolution of the eclipse environment.

2.2 Probing eclipse mechanism for PSR J1431–4715

We obtained the lower limit of the N_e and the eclipse radius (R_c) for PSR J1431–4715 to be $9 \times 10^{-17} \text{ cm}^{-2}$ and $2.7 \times 10^{11} \text{ cm}$ respectively, as evident from Figure 2. We estimated the volume electron density in the eclipse medium $n_e = N_e/R_c$ to be $3.3 \times 10^6 \text{ cm}^{-3}$. In the following, we applied the mechanism detailed by (5) to PSR J1431–4715. First is the plasma frequency cut-off. If the frequency of the radio waves is lower than the plasma frequency in the eclipse medium, they would not be able to propagate through it. We estimated the maximum n_e in the eclipse region to be $3.3 \times 10^6 \text{ cm}^{-3}$, and using this value of n_e , the plasma frequency cut-off is $f_p = 8.5 \left(\frac{n_e}{\text{cm}^{-3}} \right)^{1/2} \text{ kHz} = 15.44 \text{ MHz}$. The obtained value of the plasma frequency is far less than the observed ν_c . Second is the eclipse due to refraction. This can be ruled out as the observed delays are in microseconds (μs), whereas the required delay for refraction to be the main eclipse mechanism should be in milliseconds (5). Next is scattering. Scattering of radio waves will give rise to pulse broadening, and if the pulse gets broadened more than the period of the pulsar, the pulsar signal will not be detected, resulting in an eclipse. At 1251 MHz with dispersion measure (DM) = $59.34 + 0.24 \text{ cm}^{-3} \text{ pc}$ (where 59.34 is the DM of the pulsar, and 0.24 is the excess DM (DM_{excess}) in the eclipse region), the increase in pulse width as a result of scattering (22) is 0.000645 ms, which is much less than the pulse width of the pulsar (0.4 ms, assuming a duty cycle of 20%). Therefore, scattering cannot explain the eclipse at 1251 MHz. Eclipse due to free-free absorption can also be ruled out. Solving for the optical depth (τ_{ff}) equation with $\tau_{ff} = 1$ gives the condition $T \leq 11740 f_{cl}^{2/3}$, where T is the temperature in the eclipse medium and f_{cl} is the clumping factor. For the above condition to be satisfied, either very low temperatures or very high clumping factors are required, both of which are practically not feasible in the eclipse region, as the pulsar radiation is itself intense enough to heat the plasma beyond this required temperature value. Eclipse because of induced Compton scattering can also be ruled out as the obtained optical depth for induced Compton scattering is less than 1. Eclipse due to cyclotron absorption can also be ruled out, as for cyclotron absorption to be valid, temperatures above 10^7 K in the eclipse medium are required, whereas cyclotron absorption is valid for $T < 1.9 \times 10^5 \text{ K}$. Therefore, we conclude that for PSR J1431–4715, synchrotron absorption is the major eclipse mechanism, as seen for many other BW MSPs (7; 6; 8).

2.3 Unusual increase in the total intensity in the eclipse phase for PSR J0024–7204

We also examined the intensity as a function of orbital phase to investigate evidence of eclipsing. For PSR J0024–7204, only on October 16, 2020, did we observe a slight reduction in flux density (not completely zero) around superior conjunction (\sim orbital phase 0.25), using only the lower part (~ 700 – 1107 MHz) of the UWL band. In other epochs for this pulsar, we did not observe a decrease in total intensity near orbital phase 0.25. On July 8, 2019, two consecutive eclipses are covered. For the first eclipse, we observed an increase in flux density in the eclipse region, despite the presence of extra material in this region (indicated by DM_{excess} and N_e) as shown in Figure 1. However, for the second eclipse covered, we did not observe an increase in flux density in the eclipse region. This increase in flux density during the eclipse phase is unusual and not seen for BW MSPs in general and could be the first detection of plasma lensing in PSR J0024–7204. Previous studies have reported plasma lensing in black widow MSPs. For example, (13), (25), and (24) observed plasma lensing in PSR J2051–0827, J1959+2048, and PSR B1744–24A, respectively.

For PSR J1431–4715, we also carried out a similar study of intensity versus orbital phase and observed a decrease in intensity in the eclipse region which is in agreement with other BW MSPs.

3 Depolarisation of pulses in the eclipse phase

Efforts have been made in the past to determine the magnetic field in the eclipse region for spider MSPs. However, until now, it has only been possible to ascertain the magnetic field at the eclipse boundary, not at its center. For instance, in a recent study by (13), the magnetic field for J2051–0827 was estimated to be 0.1 G. Meanwhile, using the plasma lensing technique, a study by (14) estimated the magnetic field for PSR J1959+2048 to be less than 0.02 G. The expected magnetic field (characteristic magnetic field estimated by pressure balance between the pulsar energy density and the stellar wind energy density of the companion) at the eclipse center is approximately 10 G. The difference between the observed and expected values might arise because the magnetic field measured by (14) and (13) is not at the eclipse center, but is measured at the eclipse boundary. The reason for the non-detection of magnetic field at the eclipse centre could be either that the cutoff frequency for that particular pulsar exceeds the observing band or that signal depolarization is observed during the eclipse phase. Depolarization refers to the decrease in the linear polarization percentage of radio waves as it passes through an intervening medium.

Depolarization during the eclipse phase has been observed in spider MSPs. For example, depolarization in the eclipse medium is observed for PSR J2051–0827 by (13), for PSR J2256–1024 by (15), and for J1748–2446A by (16).

Table 1. Table listing the cut-off frequency values for multiple observing epochs along with corresponding electron column density.

| Pulsar name | Date | Cut-off frequency(ν_c) | Eclipse orbital phase ^a | N_e^b (cm^{-2}) | Frequency ^c (MHz) |
|-------------|-------------------------|------------------------------|------------------------------------|------------------------------|------------------------------|
| J0024–7204 | 16-08-2020 | < 734 | 0.22–0.26 | 3×10^{16} | 734–1107 |
| | 27-01-2021 | < 1911 | 0.22–0.26 | 4×10^{16} | 1911–2221 |
| | 29-05-2019 | < 1232 | 0.22–0.26 | 5×10^{16} | 1232–1655 |
| | 08-07-2019 ¹ | < 734 | 0.18–0.21 | 1×10^{16} | 734–1107 |
| | 08-07-2019 ² | < 734 | 0.18–0.21 | 2×10^{16} | 734–1107 |
| | 14-07-2019 | > 1581 | 0.22–0.26 | $4 \times 10^{16*}$ | 1251–1581 |
| J1431–4715 | 2019-02-13 | 1251 | 0.22–0.25 | $9 \times 10^{17*}$ | 1251–1600 |
| | 2019-06-07 | 1251 | 0.28–0.30 | $9 \times 10^{17*}$ | 1251–1600 |

^a: The orbital phase taking which the precise or constrain on the cut-off frequency is obtained; ^b: The maximum electron density in the eclipse medium; ^c: Frequency chunk that has been considered to find the maximum value of N_e in the eclipse medium; *: The epochs where only the limit on the N_e is known; ¹: 1st orbit; ²: 2nd orbit.

Small-scale spatial fluctuations in electron density or magnetic field in the eclipse medium can result in rapid temporal variations in RM and averaging over a few sub-integrations can lead to depolarization (16).

We investigated how the RM changes with orbital phase for PSR J0024–7204J and J1431–4715, as we observed good fractional linear polarization for these two systems. For PSR J0024–7204J, Figure 1 depicts the RM variation with orbital phase. Notably, except for the point at orbital phase 0.65, the RM value decreases until the eclipse ingress. In the eclipse region, no determination of RM is possible, as the pulsar undergoes depolarization. In previous studies, the RM for this pulsar has been determined using different radio telescopes. With the MeerKAT telescope, an RM value of $+24 \text{ rad/m}^2$ was obtained after excluding the eclipse phase (17). A study by (18), using the central beam of the Parkes Multi-Beam Receiver with a central frequency of 1382 MHz and a bandwidth of 400 MHz, reported an RM value of -9 rad/m^2 for this pulsar. Another study using the Parkes UWL receiver data yielded an RM value of $+20 \text{ rad/m}^2$ (19). However, it remains uncertain whether the eclipse phase was excluded in both of the above Parkes observations when calculating the RM value. We utilized the data set from (19) to investigate the orbital phase dependent RM variations, that was not explored by the authors.

For PSR J1431–4715, we obtained a consistent RM value around 30 rad/m^2 throughout the orbit, except during the eclipse phase. During this specific orbital phase, we observed the depolarization of pulses for this pulsar. A previous polarization study of this pulsar was conducted using the MeerKAT radio telescope, revealing an RM value of 13.3 rad/m^2 (20). However, whether this value was obtained by excluding the eclipse phase is not mentioned in their study.

The duration of depolarization for J0024–7204 (approximately from 1.0 ± 0.05 to 1.5 ± 0.05 orbital phase in Figure 1) at 921 MHz (with a bandwidth of 374 MHz) is almost similar to what is observed for PSR J1431–4715 (approximately 0.1 ± 0.03 to 0.43 ± 0.03 orbital phase in Figure 2) at 993 MHz (with a bandwidth of 517 MHz). The depolar-

ization duration could be more for PSR J1431–4715, as the orbital phase between 0.0 and 0.1 is not covered by observations. Considering the random RM variations following a normal distribution with a standard deviation of σ_{RM} , the ratio of the observed linear polarisation (L_{obs}) to the actual linear polarisation (L) is given as, $L_{obs}/L = e^{-2\sigma_{RM}^2/\lambda^4}$ (21). For the L_{obs} to be less than 1% of the L , σ_{RM} values greater than 95 rad/m^2 at 921 MHz and 123 rad/m^2 at 993 MHz are required. RM variations with σ_{RM} greater than these values at the mentioned frequencies in the eclipse region would lead to depolarization, with the depolarization mechanism becoming more pronounced at longer wavelengths or shorter frequencies.

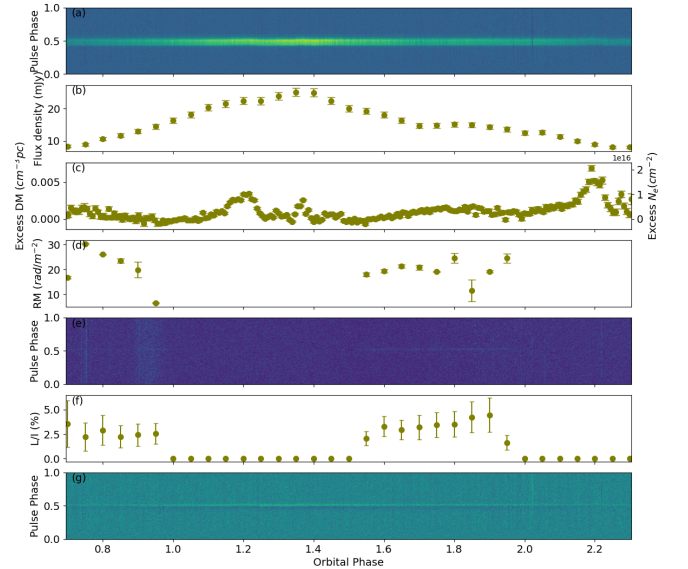


Figure 1. Seven panels depict, from top to bottom, (a) the total intensity, (b) flux density of total intensity, (c) excess DM, (d) RM, (e) linear polarization intensity, (f) linear polarization fraction percentage, and (g) circular polarization intensity variation with orbital phase for PSR J0024–7204 on 8th July 2019. The above quantities have been calculated for the 734–1107 MHz frequency range.

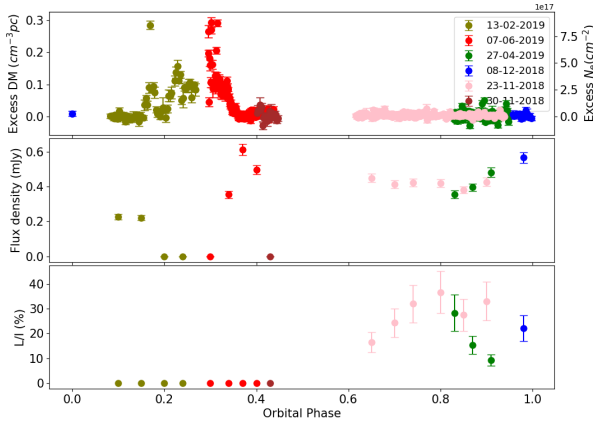


Figure 2. The topmost, middle, and bottom plots depict variations in DM_{excess} , flux density, and linear polarization fraction percentage (L/I) with orbital phase for PSR J1431–4715. Different colors represent different epochs of observations. The DM_{excess} variation is determined using the 1251–1600 MHz frequency range, given that the cut–off frequency for this pulsar is 1251 MHz. The flux density and linear polarization fraction percentage are estimated using the 734–1251 MHz frequency range.

4 Summary

This paper presents the cut–off frequency and orbital phase-dependent polarization study for PSR J0024–7204 and PSR J1731–4715, respectively. We concluded that the eclipse cut–off frequency for both pulsars could be varying with time, along with the temporal variation of N_e in the eclipse region. Such variations could indicate that the eclipse environment is dynamically evolving, as observed for PSR J1544+4937 by (10). Using the cut–off frequency estimate of 1251 MHz for PSR J1731–4715, we concluded that synchrotron absorption by trans-relativistic free electrons in the eclipse medium is the major eclipse mechanism. Additionally, we observed an unusual increase in total intensity in the eclipse region for PSR J0024–7204, which is generally not seen for other BW MSPs. In other BW MSPs, a reduction of total intensity in the eclipse region is observed in previous studies. In the orbital phase-dependent polarization study, we observed the depolarization of pulses in the eclipse phase. The cause of this depolarization could be rapid fluctuations of RM in the eclipse medium.

References

- [1] Fruchter, A. S., Stinebring, D. R., & Taylor, J. H. 1988, *Nature*, 333, 237
- [2] Roberts, M. S. 2012, *Proceedings of the International Astronomical Union*, 8, 127
- [3] Polzin, E. J., Breton, R. P., Stappers, B. W., et al. 2019, *MNRAS*, 490, 889
- [4] You, X. P., Manchester, R. N., Coles, W. A., Hobbs, G. B., & Shannon, R. 2018, *ApJ*, 867, 22
- [5] Thompson, C., Blandford, R. D., Evans, C. R., & Phinney, E. S. 1994, *ApJ*, 422, 304
- [6] Kudale, S., Roy, J., Bhattacharyya, B., Stappers, B., & Chengalur, J. 2020, *ApJ*, 900, 194
- [7] Kansabanik, D., Bhattacharyya, B., Roy, J., & Stappers, B. 2021, *The Astrophysical Journal*, 920, 58
- [8] Polzin, E. J., Breton, R. P., Clarke, A. O., et al. 2018, *MNRAS*, 476, 1968
- [9] Polzin, E. J., Breton, R. P., Stappers, B. W., et al. 2019, *MNRAS*, 490, 889
- [10] <https://arxiv.org/pdf/2311.02071.pdf>
- [11] Freire, P. C. C. 2005, in *Astronomical Society of the Pacific Conference Series*, Vol. 328, *Binary Radio Pulsars*, ed. F. A. Rasio & I. H. Stairs, 405
- [12] Miraval Zanón, A., Burgay, M., Possenti, A., & Ridolfi, A. 2018, in *Journal of Physics Conference Series*, Vol. 956, *Journal of Physics Conference Series*, 012004
- [13] Wang, S. Q., Wang, J. B., Li, D. Z., et al. 2023, *ApJ*, 955, 36
- [14] Li, D., Lin, F. X., Main, R., et al. 2019, *MNRAS*, 484, 5723
- [15] Crowter, K., Stairs, I. H., McPhee, C. A., et al. 2020, *MNRAS*, 495, 3052
- [16] You, X. P., Manchester, R. N., Coles, W. A., Hobbs, G. B., & Shannon, R. 2018, *ApJ*, 867, 22
- [17] Abbate, F., Possenti, A., Ridolfi, A., et al. 2023, *MNRAS*, 518, 1642
- [18] Abbate, F., Possenti, A., Tiburzi, C., et al. 2020, *Nature Astronomy*, 4, 704
- [19] Zhang, L., Hobbs, G., Manchester, R. N., et al. 2019, *ApJL*, 885, L37
- [20] Spiewak, R., Bailes, M., Miles, M. T., et al. 2022, *PASA*, 39, e027
- [21] Li, D., Bilous, A., Ransom, S., Main, R., & Yang, Y.-P. 2023, *Nature*, 618, 484
- [22] Bhat, N. D. R., Cordes, J. M., Camilo, F., Nice, D. J., & Lorimer, D. R. 2004, *ApJ*, 605, 759,
- [23] Lin, F. X., Main, R. A., Verbiest, J. P. W., Kramer, M., Shaifullah, G. 2021, *MNRAS*, 506, 2824
- [24] Bilous, A. V., Ransom, S. M., Demorest, P. 2019, *ApJ*, 877, 125
- [25] Main, R., Yang, I. S., Chan, V., et al. 2018, *Nature*, 557, 522